Jurnal Ilmu Fisika

Open Access

JURNAL ILMU FISIKA
JIF
UNIVERSITAS ANDALAS

Synthesis of Supercapacitor from Cocoa Fruit Peel Activated Carbon for Energy Storage

Rahma Fikri Nuradi[1], Mulda Muldarisnur[1], Yuli Yetri[2]

[1] Department of Physics, Faculty of Mathematics and Natural Sciences, Universitas Andalas, Padang, 25163, Indonesia
[2] Department of Mechanical Engineering, Politeknik Negeri Padang, Padang, 25163, Indonesia

Article Info	ABSTRACT
  Corresponding Author: Yuli Yetri E-mail: yuliyetri@pnp.ac.id	The supercapacitor electrode has been synthesized using activated carbon from cocoa pods. Activated carbon was prepared by first drying the raw materials under the sunlight and followed by oven drying, pre-carbonization, milling, sieving, and chemical activation with 0.3 M and 0.4 M KOH solution. After chemical activation, the activated carbon was printed into pellet form, carbonized at a temperature of 600 °C, followed by physical activation at a temperature of 700 °C for four hours before polishing. We found that the optimum conditions are 700 °C and 0.4 M. The density of the obtained carbon electrode is 0.810 g/cm³. The SEM micrographs show the formation of pores with a diameter of 0.44 μm and 0.98 μm. The carbon content in the electrode sample measured using electron dispersive spectroscopy is 91.49%. The XRD data shows that the carbon electrode is amorphous with a diffraction angle (2θ) at 23.569° and 44.781°. The optimum specific capacitance of the supercapacitor is 140.2 F/g obtained for the sample activated for 2.5 hours. *Copyright © 2022 Author(s)*

1. INTRODUCTION

One of the energy storage media currently being intensively investigated is capacitors and supercapacitors. Supercapacitors, also known as electrochemical capacitors, are electrical double layers in the form of electrodes separated by a separator (Boyea et al., 2007). Supercapacitors are electrochemical devices that can rapidly store and discharge electrical charges at high power densities. The charge storage capacity of supercapacitors is a thousand times higher than that of conventional capacitors. The time required to recharge a supercapacitor with a capacity of hundreds of Farads is only 30 seconds. Supercapacitors consist of carbon with a very active surface area called activated carbon and a thin layer of electrolyte that acts as a dielectric and charge separator. An essential component of a supercapacitor is electrodes (i.e., an anode and a cathode). The choice of electrode material determines the performance of the supercapacitor significantly.

In order to achieve much higher specific capacitance compared to the conventional capacitors, supercapacitor electrodes have been made using carbon aerogel (Liu et al., 2013), nanocomposites (Rosi et al., 2013), metal oxides (Ferreira et al., 2014), and conductive polymers (Rosi et al., 2014). The materials mentioned above are rare, expensive, and challenging to synthesize. Sustainability and environmental friendliness are the main driving force for researchers to use organic materials as a future energy source in realizing green technology (Tetra et al., 2018).

Currently, the most widely developed electrode materials are carbon and its composites. Activated carbons are widely used in various electrochemical applications such as in petroleum fertilizer plants, pharmaceuticals, textiles, automobiles, adsorbents, and many others (Tadda et al., 2016). Activated carbon is used because it is cheap, the essential ingredients are easy to obtain, easy to synthesize, can be made in many forms (powder, fiber, and composites), and has a large surface area with adjustable porosity. Carbon electrodes are easily polarized, stable in different solutions (acids, bases, and aprotic), and stable in a specific temperature range (Frackowiak, 2006).

Organic materials have a high carbon content, which is the most critical factor determining a supercapacitor's ability to store electric charges. Supercapacitors have been fabricated using various organic materials such as elephant grass flowers (Taer et al., 2016), rubber wood sawdust (Taer et al., 2016), rubber wood (Muchammadsam et al., 2015), durian skin (Taer et al., 2018), banana stem waste (Taer et al., 2018), and sago pulp (Afrianda et al., 2017). Each of these materials has a different specific capacitance. The highest specific capacitance of sago dregs is 132.09 F/g, rubber wood is 115 F/g, banana stem waste is 104 F/g, rubber wood sawdust is 50.65 F/g, durian skin is 66 F/g, and elephant grass flower is 43 F/g. Sago dregs are pretty challenging to obtain and only found in certain areas, so other agricultural waste alternatives must be developed.

One of the agricultural wastes that can be used as a supercapacitor is cocoa pods. Cocoa pods contain hemicellulose 21.06%, cellulose 20.15%, and lignin 51.98% (Wijaya and Wiharto, 2017). The specific capacitance of chemically-activated cocoa pods with KOH at 0.4 M at 700 °C is 140.2 F/g, which is higher than that activated with 0.3 M at 700 °C (e.g., 90.2 F/g). This result shows that the cocoa pod skin can be used as a raw for the fabrication of supercapacitors (Yetri et al., 2020). The results mentioned above encourage us to develop and refine electrodes from cocoa pods to fabricate supercapacitors using cocoa pod shell waste. So far, it has not been utilized optimally; therefore, it has low economic value.

2. MATERIALS AND METHOD

2.1 Materials

Cocoa is the main material for fabricating the supercapacitor electrode in this work. Cocoa (*Theobroma cacao*) seeds in the form of fresh fruit consist of 73% fruit skin, 2% placenta, and 24.2% seeds. Cocoa pods contain 32.3% carbohydrates, 21.44% lignin, 19.2% sugar, 8.6% protein, and 27.7% minerals. Therefore, selecting cocoa pods as a raw material in the fabrication of supercapacitor electrodes can help the processing of cocoa pod waste that has not been fully utilized. Supercapacitor electrodes were prepared using a cocoa pod, calcium hydroxide, polyvinyl alcohol, filter paper, and copper plate.

2.2 Electrode preparation

The production of activated carbon from cocoa pod biomass started with the selection of fresh, clean, and not rotten cocoa pods. Cocoa skin was cut into thin pieces with a dimension of 5 cm ×1 cm. The cut cocoa pods were dried indoors until the moisture content was reduced by about 85%. The following process was pre-carbonization which was carried out at a temperature of 250 °C in a vacuum for 2.5 hours. The process is as follows: 50 grams of dry cocoa pods were put in a stainless-steel tube, then put in an oven with an initial temperature of 50 °C, and then the temperature was increased by 50 °C every 30 minutes to a maximum value of 250 °C. The dark brown cocoa pod skin from the pre-carbonization process has a carbon content of approximately 70% and has an average mass loss of 25.3%, which is brittle, so it is easy to purify. The following process was crushing using a milling tool. The process was as follows: 150 grams of pre-carbonized sample was put into a cup and ground until the sample was very fine. The carbon sample was then sieved through a 38 μm sieve to obtain particles of less than 38 μm. The next stage was the activation process with 0.3 M and 0.4 M KOH. Afterward, the beaker was placed on a hot plate using a magnetic stirrer at 80 °C for one hour. The cocoa pod powder was added and stirred until well blended. Then it was left for two hours at a constant temperature

of 80 °C. Then, the hot plate was switched off to allow the sample temperature to drop to room temperature (30 °C). The pre-carbonized cocoa powder was washed with distilled water until a neutral pH was obtained. The samples were dried in an oven at 105 °C for 24 hours. The dry sample was ground again with a grinding mortar and sieved to its original size, then weighed with a mass of 0.7 g until it was molded into pellets.

The molding of carbon pellets was carried out using a hydraulic press at a pressure of 8 tons. The next stage is the carbonization process using the Payun Tech furnace, starting at room temperature and allowed to rise to 305 °C for 1 hour. Continued to a maximum temperature of 600 °C in the nitrogen gas environment and continued with physical activation at a temperature of 700 °C using CO2 gas. The temperature of 305 °C was measured from the skin temperature of the durian fruit because the skin of the cocoa and durian fruit has the same texture after the dehydration process (Taer et al. 2018).

2.3 Electrochemical characteristics

Measurement of the dimensions of the cocoa pod pellets included measurements of mass, diameter, and thickness of each pellet before and after carbonization-physical activation. Data density is calculated using the formula in equation (1).

$$\rho = \frac{m}{V} \tag{1}$$

where ρ is the density, m is the mass, and V is the volume of the carbon pellet. After measuring the density, the carbon pellet samples were polished with a diameter of 8 mm and a thickness of 0.3 mm, then washed until the pH of the washing water became neutral. Next, the electrode-neutralized carbon was immersed in a 1 M sulfuric acid (H_2O_4) solution, which served as the electrolyte in the supercapacitor cell. The electrochemical properties of the carbon electrodes were tested by assembling a supercapacitor cell. The supercapacitor cells are assembled in the shape of a coin in which a pair of carbon pellets are used as electrodes and attached to a stainless-steel current collector and bounded by an insulating material from the eggshell membrane. The specific capacitance of the supercapacitor can be measured using the cyclic voltammetry (CV, UR Rad-Er 5841) at an induction rate of 1 mV/s to 100 mV/s. The specific capacitance can be calculated using equation (2) (Yusriwandi et al., 2017).

$$C_{sp} = \frac{I_c - (-I_d)}{s \cdot m} \tag{2}$$

where C_{sp} is the specific capacitance, I_c is the charge current, I_d is the discharge current, s is the scanning rate, and m is the mass of the activated carbon electrode.

## 2.4 Physical Characteristics

In addition to chemical composition, dimensions, mass, crystallinity, and morphology of monolithic activated carbon samples produced from cocoa pods were measured. The mass and dimensions of the samples were documented to determine the monolith density of activated carbon samples under KOH concentration. The Philip X-Pert Pro PW 3060/10 device based on a Cu k-α light source and operated at a wavelength of 1.5418 Å was used to investigate X-ray diffraction (XRD) in order to understand the crystallinity of activated carbon samples. The diffraction angle ranging from 10-100° was used to examine the diffractogram. The Bragg equation is used to calculate the distance between layers (d_{hkl}) (Fuhu et al., 2010), while the peaks obtained from the measurement data were then matched with standard X-ray diffraction for almost all types of materials. This standard is called JCPDS-ICDD (Joint Committee on Powder Diffraction Standard-International Center for Diffraction Data) (Clearfield et al., 2008). Scanning electron microscopy (SEM) at magnification and energy of 5000 dispersive spectroscopy (EDX) with the support of the JEOL JSM-6510 LA device was also used to test the surface morphology and chemical composition. A Quanta chrome Nova Win Instrument version 11.0 based on the isothermal adsorption-desorption method of nitrogen gas (N_2) was operated to analyze the surface area.

3. RESULTS AND DISCUSSION

The physical properties of supercapacitor electrodes can be seen in the measurement of mass (m), diameter (d), thickness (t), and density (ρ) for each variation before and after carbonization-physical activation. The process of losing the sample's mass, diameter, and thickness causes a decrease in density. The density of the samples after carbonization and activation are presented in Table 1. The activation process of carbonization at each concentration variation causes the dimensions and density of the carbon pellets to shrink. The increase in KOH concentration from 0.3 M to 0.4 M also causes a decrease in the dimensions and density of carbon pellets. These results are in accordance with previous research (Taer et al., 2018) on manufacturing electrode supercapacitors from rubber wood using chemical activation of KOH and Nitric Acid (HNO_3), confirming that the density value of carbon electrodes decreased after activation. The reduction in density at the carbon electrode is due to the addition of the pore structure due to combination activation (Farma et al., 2013).

Table 1 Mass, diameter, thickness, and density before and after physical activation 700 ºC

| Concentration	Sample	m (g)	d (cm)	t (cm)	ρ (g/cm^3)
0.3 M	Pre-carbonization	0.703	1.985	0.254	0.918
	After activation	0.256	1.480	0.187	0.850
0.4 M	Pre-carbonization	0.689	1.978	0.240	0.950
	After activation	0.230	1.483	0.179	0.801
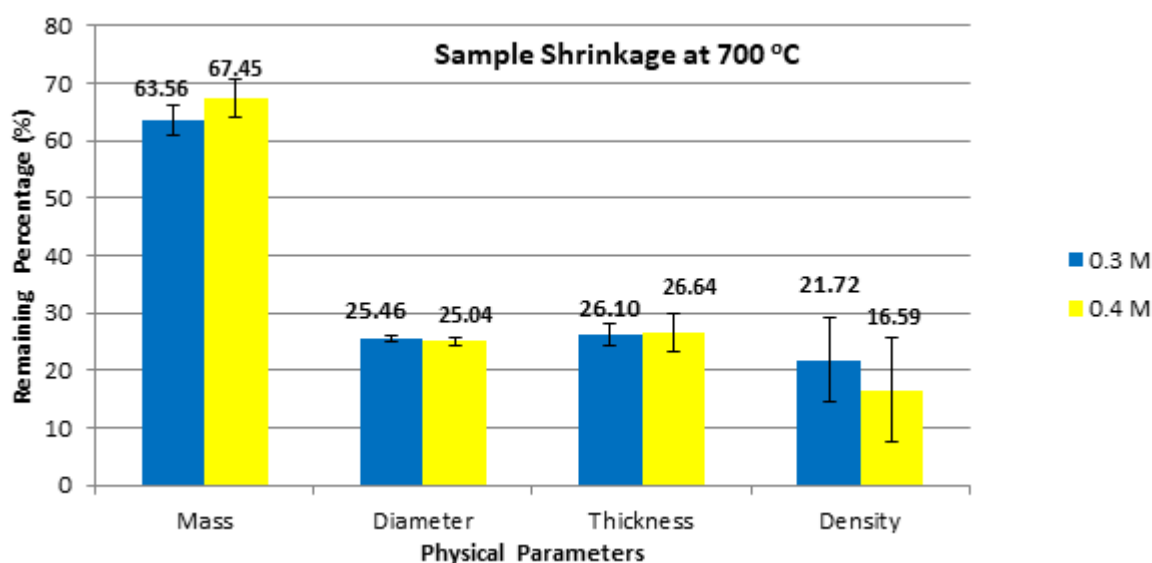
Figure 1 Percentage of mass, diameter, thickness, and density of pre-carbonized and physically activated carbon at 700 °C with KOH 0.3 M and 0.4 M.

Figure 1 shows the percentage of carbon pellets' mass shrinkage, diameter, thickness, and density. The mass loss that occurs in the 0.4 M sample with an activation temperature of 700 °C is greater than the mass loss in the 0.3 M sample with the same activation temperature, although it is not very significant. The carbonization and activation processes induce the decomposition of organic materials in the cocoa pods and release volatile substances such as water vapor. The dominant mass loss will affect the diameter and thickness shrinkage. There is a significant difference between dimensions and thickness shrinkage in the 0.3 M sample at 700 °C. The shrinkage is much more significant than that in the 0.4 M sample at the same temperature. At the same time, the diameter is more or less similar. Density reduction occurs at the electrodes. The combination of the activation process increases carbon pore structure

(Basri et al., 2016). The highest shrinkage occurred in the sample mass caused by the evaporation of materials other than carbon during the carbonization and activation process. Carbonization and physical activation are followed by carbon chaining to form more complex compounds.

Furthermore, the evaporation of the non-carbon material causes an increase in the pore size. It generates new pores in the electrode, resulting in particles becoming brittle, breaking, and breaking. The splitting of particles into finer particles will cover the pores that have been formed so that the density of the sample will increase (Taer et al., 2018). This phenomenon causes the carbon monolith's mass to shrinkage and increases the sample's porosity. The shrinkage in diameter and thickness is also caused by direct heating.
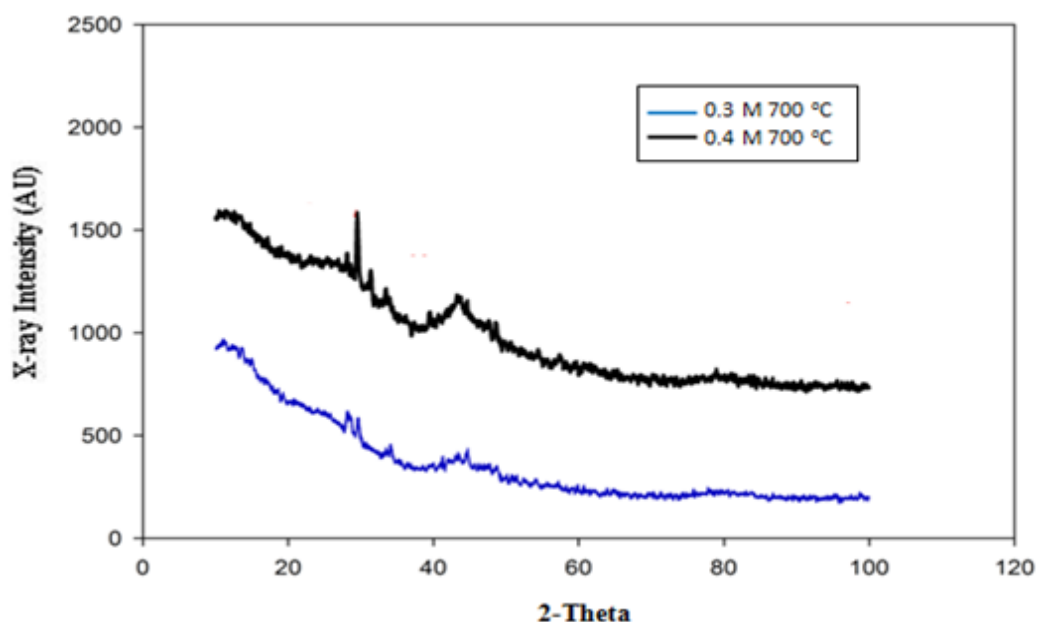
Figure 2 Diffraction pattern of cocoa pod biomass after chemical activation.

3.1 XRD analysis

X-ray diffraction was carried out to determine the lattice parameters, crystal size, and crystal phase formed on the carbon electrode. The diffraction angle was 2θ in the range of 10-100°. The XRD carbon pattern of cocoa pod biomass with chemical activation variations of 0.3 M and 0.4 M KOH is shown in Figure 2. The graph shows the relationship between X-ray intensity and scattering angle (2θ) in both carbon samples from cocoa pods. There are two broad peaks with an angle of 2θ from 25 to 35, corresponding to the (002) and (100) diffraction planes. The fitting results obtained data from the scattering angle, peak height, and width. The angle at each peak was determined using Microcal Origin software. Data fitting of X-ray diffraction data on the cocoa pod skin electrode can be seen in Table 2.

Table 2. Data fitting of X-ray diffraction data on the cocoa pod skin electrode.

Sample code	2θ	θ	h	k	l	d (Å)	a (nm)
700 °C 0.3 M	28.1233	14.06165	1	1	1	317.302	54.958319
	29.5897	14.79485	1	1	1	301.903	52.291133
700 °C 0.4 M	29.4921	14.74605	1	0	4	30.263	12.477755
	31.3901	15.69505	1	1	1	28.521	49.399821

The difference in the electrode structure of 0.3 M 700 °C and 0.4 M 700 °C can be observed from the XRD diffractogram peak height data, namely 91.98 nm for the 0.3 M 700 °C sample, for the

0.4 M 700 °C sample, it is 320.64 nm, From the two samples, it was obtained that the sample with the highest peak height was 0.4 M 700 °C at 320.64 nm. The shift in peak height and peak width at half height indicates the rearrangement of carbon atoms. The most significant ratio number was obtained at the electrode sample of 0.3 M 700 °C. Variations in KOH concentration on chemical activation showed significant differences in the number of lattice deposits.

Based on this analysis, it can be claimed that the increase in KOH concentration led to the formation of large micropores and mesoporous, resulting in a larger surface area. This feature increases ion storage and provides rapid ion mobility for surface-activated carbon.

3.2 Scanning electron microscope (SEM) observation analysis

Scanning electron microscopy (SEM) was used to determine the morphology of the carbon electrodes made of cocoa pods and investigate pore distribution. The results of observations on samples with a magnification of 5000 times can be seen in Figure 3. Figure 3(a) shows the results of SEM of 0.3 M carbon electrode at 700 °C with a magnification of 5000 times. The surface morphology of activated carbon shows the presence of pores. The pores between the particles spread almost evenly on the sample surface, some of which are elongated and irregular.

On the sample's surface at 0.3 M at 700 °C, there are still small particles indicating the presence of non-carbon materials or free particles that did not completely evaporate during the carbonization and activation process. The particles formed are more apparent, and there are evenly distributed pores of various shapes and sizes between these particles. Figure 3(b) shows the SEM results of a 0.4 M carbon electrode at 700 °C with 5000 times magnification. Figure 3(b) shows that the pores between the particles are larger than the 0.3 M carbon electrode sample at 700 °C, the size is uneven, and the shape is irregular. Figure 3(b) also shows a cut on the surface of the carbon electrode, presenting a denser electrode sample structure. At the same time, the particles formed are clearer, and between particles, there are large pores with variable sizes. The difference between the images of the two samples is the presence of small particles covering the pores between the particles so that the pore size reduces. The closed pores cause the density of the carbon electrode to increase, resulting in a small specific capacitance (Armynah et al., 2019).
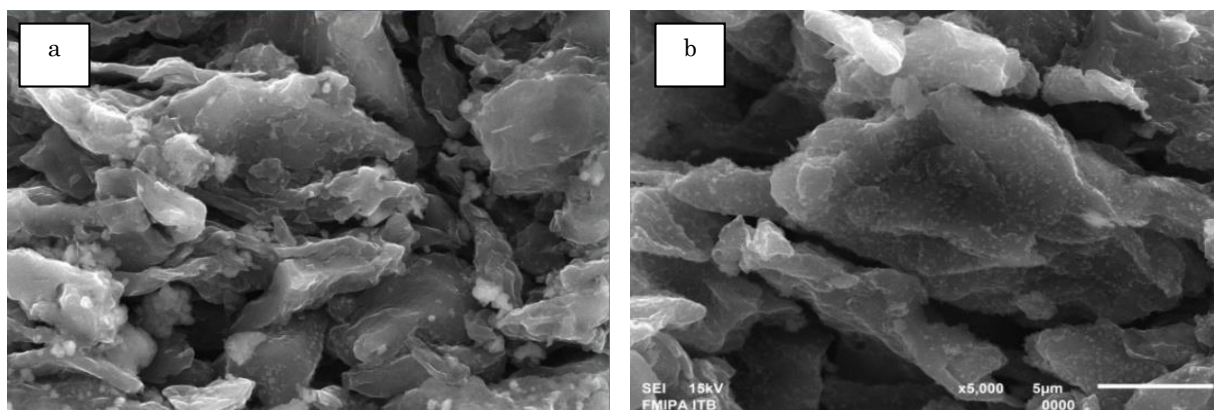
**Figure 3** SEM images of carbon electrodes (a) 0.3 M at 700 ºC, and (b) 0.4 M 700 ºC

3.3 Energy Dispersion X-ray Analysis

The X-ray dispersion energy (EDX) represents the percentage of elemental content in the electrode sample's carbon. Table 3 shows the elements in the carbon electrode sample that are carbon, oxygen, magnesium, and calcium. At the activation of 0.3 M and 0.4 M, the percentage of the carbon element content is higher, namely 91.02% at 0.3 M and 91.49% at 0.4 M. The high C content indicates that the carbon electrode sample has very high purity. Oxygen has the second-highest percentage after element C, likely due to incomplete decomposition during the carbonization process and C-O bonds in the activation process. The content of Ca in the carbon electrode is caused by essential elements in

biomass waste, including cocoa pods. Elemental Mg was shown to come from steel balls that were not cleaned during ball milling, and the presence of element K was due to the chemical activation of this compound, which did not completely decompose. The amount of element C in the sample of 0.4 M carbon electrode is greater than that of the 0.3 M carbon electrode sample at the same temperature. A concentration of 0.4 M KOH indicates more carbon than a concentration of 0.3 M for KOH. Adding KOH activator concentration from 0.3 M to 0.4 M resulted in more decomposition of non-carbon content, so the element C produced was higher.

Table 3 The content of compounds in the sample of 0.3 M and 0.4 M carbon electrodes at 700 $^{\circ}$C.

Content	0.3 M		0.4 M	
	Mass %	Atom %	Mass %	Atom %
C	87.05	91.02	87.87	91.49
O	10.12	7.95	9.65	7.54
Mg	0.75	0.39	0.94	0.48
Ca	2.07	0.65	1.55	0.48
Total	100	100	100	100
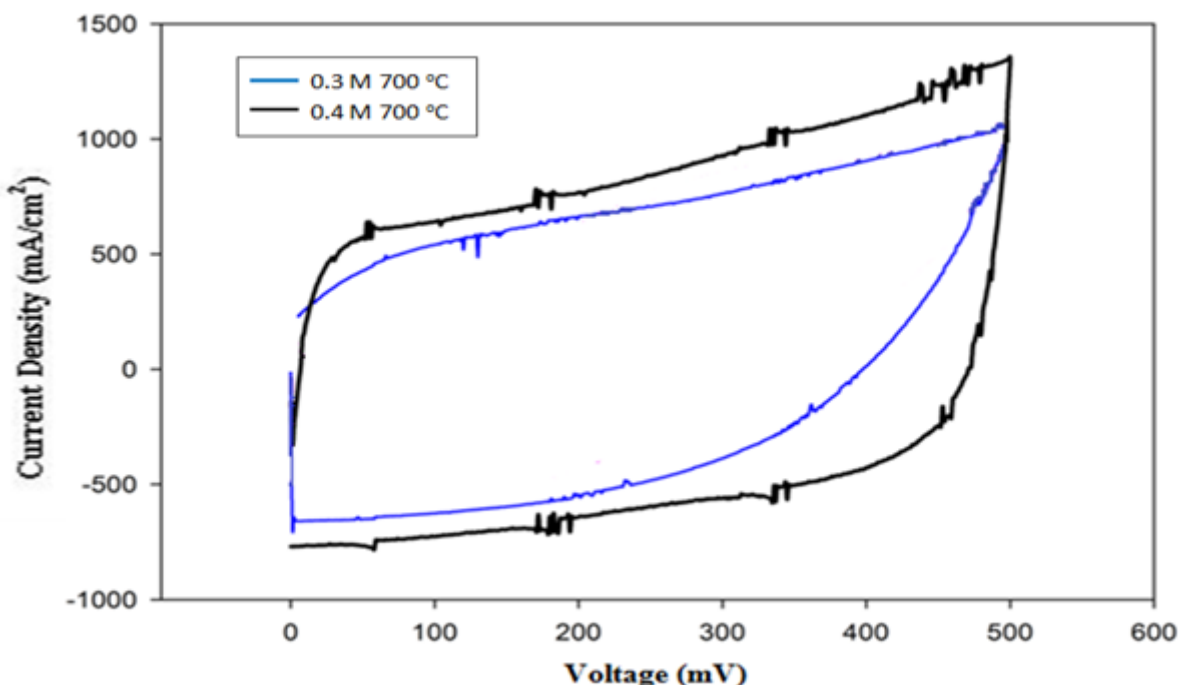
Figure 4 Curve of the relationship between specific capacitance to the voltage at a scanning rate of 1 mV

3.4 Electrochemical Properties

Cyclic voltammetry (CV) measurement data are expressed in specific capacitance (C_{sp}) curves of voltage at a scan rate of 1 mV/s. The CV curve shows the current density versus voltage for 0.3 M and 0.4 M KOH concentrations, as shown in Figure 4. The CV curve for the 0.4 M KOH treatment has a better capacitive response than that of the 0.3 M KOH sample. The better capacitive response is indicated by a broader potential of the middle region due to a large number of pores of the carbon electrode. The large number and size of pores increase the number of ions flowing to the electrode, as indicated by the width of the charge-discharge curve. Charge-discharge curve, the greater the specific capacitance generated by the activated carbon electrode. The 0.4 M carbon electrode sample at 700 °C had a better capacitive response, and it was characterized by a wider center potential area, a larger charging process at 0 V, and a horizontal shape of the discharge curve when compared to 0.3 M at 700 $^{\circ}$C. The shape of the 0.4 M CV curve at 700 $^{\circ}$C is square, which means it is the ideal shape for activated

carbon electrodes. Figure 4 shows that the addition of KOH concentration from 0.3 M to 0.4 M can increase the number of pores on the carbon electrode so that the number of ions flowing to the electrode increases, marked by the width of the charge-discharge curve. The specific capacitance increases with the increase in KOH concentration from 0.3 M to 0.4 M. The specific capacitance of 0.4 M at 700 $^{\circ}$C was significantly higher at 140.2 F/g from 0.3 M is 90.2 F/g due to its large surface area and higher carbon content. As previously discussed, a large surface area is beneficial for increasing contact and accumulation of more electrolytes, resulting in a high charge storage density (Wang et al., 2012). Table 4 shows the specific capacitance values based on variations in KOH concentration.

Table 4 Specific capacitance values based on variations in KOH at temperature of 700 $^{\circ}$C

Treatment	Electrode	Mass (g)	Average mass (g)	I_c (μA)	I_d (μA)	C_{sp} (F/g)
0.3 M	C37-4	0.0135	0.0132	707	-483	90.2
	C37-5	0.0129				
0.4 M	C47-2	0.0103	0.0112	993	-577	140.2
	C47-3	0.0121				

4. CONCLUSION

In this study, we show the potential of cocoa pods as an electrode for supercapacitors. The results indicate that the synthesis of activated carbon from cocoa pods agrees with the results of the physical and electrochemical characterization of the supercapacitor electrodes. Analysis of the dimensions, density, and specific capacitance of the supercapacitor made of cocoa pod carbon electrodes based on variations in concentration showed that the diameter and thickness of the carbon electrode pellets decreased. The most dominant mass shrinkage causes a decrease in the value of the carbon electrode density. The addition of KOH concentration also causes a decrease in the density value of 0.850 g/cm^3 for 0.3 M KOH and 0.802 g/cm^3 for 0.4 M KOH. X-ray diffraction data shows that the sample 0.4 M has a smaller lattice distance (unit cell) than the 0.3 M, indicating a larger surface area. The specific capacitance increases with KOH concentration from 0.3 M to 0.4 M, where the specific capacitance of the sample activated using 0.3 M KOH is 90.2 F/g and for the sample with 0.4 M is 140.2 F/g. These results indicate the great potential of cocoa pods as raw materials for activated carbon in the form of monoliths to improve the performance of supercapacitors. In the initial test, pellets with a diameter of 10 mm and a thickness of 1 mm result in a voltage of about 1 volt with a maximum capacitance of 140.2 F/g.

REFERENCES

Afrianda, A., Taer, E. & Taslim, R. (2017). Pemanfaatan Ampas Sagu Sebagai Elektroda Karbon Superkapasitor. *Jurnal Komunikasi Fisika Indonesia,* 14(2), 1119-1124.

Armynah, B., Taer, E., Djafar, Z., Piarah, W. H. & Tahir, D. (2019). Effect of temperature on physical and electrochemical properties of the monolithic carbon-based bamboo leaf to enhanced surface area and specific capacitance of the supercapacitor. *Int. J. Electrochem. Sci.,* 14, 7076–7087.

Basri, N. H., Deraman, M., Suleman, M., Nor, N. S. M., Dolah, B. N. M., Sahri, M. I. & Shamsudin, S. A. (2016). Energy and Power of Supercapacitor Using Carbon Electrode Deposited with Nanoparticles Nickel Oxide. *Int. J. Electrochem. Sci.,* 11, 95 – 110.

Boyea, J. M., Camacho, R. E., Turano, S. & Ready, W. J. (2007). Carbon Nanotube-Based Supercapacitors: Technologies and Markets. *Nanotechnology Law and Business,* 4(1), 585 -593.

Clearfield, A., Reibenspies, J. H. & Bhuvanesh, N. (2008). *Principles and applications of Powder Diffraction.* Singapore, John Wiley and Sons.

Farma, R., Deraman, M., Awitdrus, A., Talib, I. A., Taer, E., Basri, N., Manjunatha, J. G. G., Ishak, M., Dolah, B. N. M. & Hashmi, S. A. (2013). Preparation of highly porous binderless activated carbon electrodes from fibres of oil palm empty fruit bunches for application in supercapacitors. *Bioresource Technology,* 132, 254–261.

Ferreira, C. S., Passos, R. R. & Pocrifka, L. A. (2014). Synthesis and Properties of Ternary Mixture of Nikel/Cobalt/Tin Oxides for Supercapacitor. *Power Sources,* 271, 104-107.

Frackowiak, E. (2006). Supercapacitors Based on Carbon Materials and Ionic Liquids. *J. Braz. Chem. Soc.,* 17(6), 1074-1082.

Fuhu, L., Weidong, C., Zengmin, S., Yixian, W., Yunfang, L. & Hui, L. (2010). Activation of mesocarbon microbeads with different textures and their application for supercapacitor. *Fuel Processing Technology,* 91(1), 17–24.

Liu, N.-p., Shen, J., Guan, D.-Y., Liu, D., Zhou, X.-W. & Li, Y.-j. (2013). Effect Of Carbon Aerogel Activation On Electrode Lithium Insertion Performance. *Acta Phys.-Chim. Sin.,* 29(5), 966-972.

Muchammadsam, I. D., Taer, E. & Farma, R. (2015). Pembuatan dan Karakterisasi Karbon aktif Monolit dari Kayu Karet dengan variasi Konsentrasi KOH untuk Aplikasi Superkapasitor. *Jurnal Online Mahasiswa FMIPA,* 2(1), 8-13.

Rosi, M., Iskandar, F., Abdullah, M. & Khairurrijal, K. (2013). Synthesis and Characterization of Supercapacitor Using Nano-sized ZnO/Nanoporous Carbon Electrodes and PVA-based Polymer-Hydrogel Electrolytes. *Materials Science Forum,* 737, 191-196.

Rosi, M., Iskandar, F., Abdullah, M. & Khairurrijal, K. (2014). Hydrogel-Polymer Electrolytes Based on Polyvinyl Alcohol and Hydroxyethylcellulose for Supercapacitor Applications. *Electrochemical Science,* 9, 4251-4256.

Tadda, M. A., Ahsan, A., Shitu, A., Elsergany, M., Thirugnnasambantham, A., Jose, B., Razzaque, M. A. & Norsyahariati, N. D. N. (2016). A review on activated carbon: process, application and prospects. *Journal of Advanced Civil Engineering Practice and Research,* 2(1), 7-13.

Taer, E., Dewi, P., Sugianto, S., Syech, R., Taslim, R., Salomo, S., Susanti, Y., Purnama, A., Apriwandi, A., Agustino, A. & Setiadi, R. N. (2018). The synthesis of carbon electrode supercapacitor from durian shell based on variations in the activation time. *AIP Conference Proceedings,* 1927, 030026.

Taer, E., Susanti, Y., Awitdrus, A., Sugianto, S., Taslim, R., Setiadi, R. N., Bahri, S., Agustino, A., Dewi, P. & Kurniasih, B. (2018). The effect of CO_2 activation temperature on the physical and electrochemical properties of activated carbon monolith from banana stem waste. *AIP Conference Proceedings,* 1927, 030016.

Taer, E., Yusra, H., Iwantono, I. & Taslim, R. (2016). Analisa Dimensi, Densitas Dan Kapasitansi Spesifik Elektroda Karbon Superkapasitor Dari Bunga Rumput Gajah Dengan Variasi Konsentrasi Pengaktivan KOH. *Spektra: Jurnal Fisika dan Aplikasinya,* 1(1), 55-60.

Tetra, O. N., Aziz, H., Emriadi, Ibrahim, S. & Alif, A. (2018). Supercapacitors based on activated carbon and Ionic solution as electrolyte. *Jurnal Zarah,* 6(1), 39-46.

Wang, G., Zhang, L. & Zhang, J. (2012). A review of electrode materials for electrochemical supercapacitors. *Chemical Society Reviews* 41(2), 797–828.

Wijaya, M. & Wiharto, M. (2017). Karakterisasi Kulit buah kakao untuk karbon aktif dan bahan Kimia yang ramah Lingkungan. *Jurnal Kimia dan Pendidikan Kimia,* 2(1), 66-71.

Yetri, Y., Mursida, M., Dahlan, D., Muldarisnur, M., Taer, E. & Febrielviyenti, F. (2020). Analysis of Characteristics of Activated Carbon from Cacao (Theobroma cacao) Skin Waste for Supercapacitor Electrodes. *IOP Conf. Series: Materials Science and Engineering,* 990, 012023.

Yusriwandi, Y., Taer, E. & Farma, R. (2017). Pembuatan dan Karakterisasi Elektroda Karbon Aktif Dengan Karbonisasi Dan Aktivasi Bertingkat Menggunakan Gas CO_2 dan Uap Air. *Jurnal Ilmiah Edu Research,* 6(1), 21-26.